

Enhancement of the photocatalytic activity of TiO₂ through spatial structuring and particle size control: from subnanometric to submillimetric length scale

Carmela Aprile, Avelino Corma* and Hermenegildo Garcia*

Received 7th August 2007, Accepted 18th October 2007

First published as an Advance Article on the web 5th November 2007

DOI: 10.1039/b712168g

This review summarizes the physical approaches towards enhancement of the photocatalytic activity of titanium dioxide by controlling this semiconductor in a certain length scale from subnanometric to submillimetric distances and provides examples in which the photocatalytic activity of TiO₂ is not promoted by doping or changes in the chemical composition, but rather by application of physical concepts and spatial structuring of the semiconductor. Thus, encapsulation inside the micropores and cavities of zeolites (about 1 nm) renders small titanium oxide clusters with harnessed photocatalytic activity. On the other hand, nanometric titanium particles can be ordered forming structured periodic mesoporous materials with high specific surface area and well defined porosity. Titania nanotubes of micrometric length, either independent or forming a membrane, also exhibit unique photocatalytic activity as consequence of the long diffusion length of charge carriers along the nanotube axis. Finally, photonic crystals with an inverse opal structure and the even more powerful concept of photonic sponges can serve to slow down visible light photons inside the material, increasing the effective optical path in such a way that light absorption near the absorption onset of the material is enhanced considerably. All these physical-based approaches have shown their potential in enhancing the photocatalytic activity of titania, paving the way for a new generation of novel structured photocatalysts in which physical and chemical concepts are combined.

1. Introduction

Titanium dioxide is the most important photocatalyst because it exhibits a high durability, corrosion resistance and high oxidation potential of the valence band that ensures a general applicability to activate a broad range of substrates.^{1–18} However, there are important drawbacks that severely limit the application of titanium dioxide photocatalyst as a general

tool either to degrade organic pollutants in the gas or liquid phase or to perform useful transformations of organic compounds.^{1–7,17,19} One of the most important limitations is the lack of TiO₂ photocatalytic activity with visible light.^{1,20,21} The reason for this is that TiO₂ in the anatase form is a *wide band gap semiconductor* with a bandgap of 3.2 eV in most media, corresponding to an onset of the optical absorption band at about 350 nm. This onset of the TiO₂ absorption is also inadequate to achieve efficient solar light photocatalytic activity, since less than 5% of the solar light energy can be absorbed by TiO₂.

Instituto de Tecnología Química CSIC-UPV, Universidad Politécnica de Valencia, Av. De los Naranjos s/n, 46022 Valencia, Spain. E-mail: acorma@itq.upv.es, hgarcia@qim.upv.es

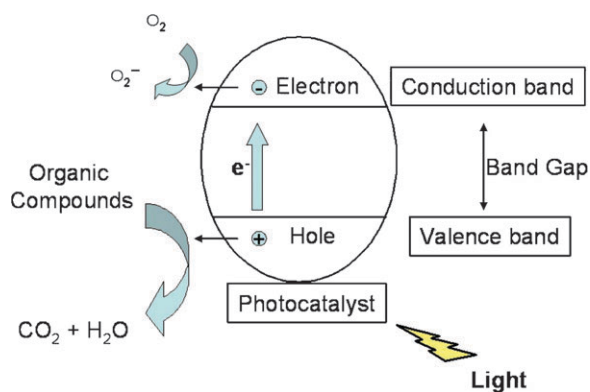


Avelino Corma was born in Moncófar, Spain in 1951. He has been the founder and director of the Instituto de Tecnología Química (UPV-CSIC) at the Universidad Politécnica de Valencia since 1990. One of his research lines is in zeolites and structured mesoporous materials, from the point of view of synthesis, characterization and reactivity. Avelino Corma is co-author of more than 700 articles and 100 patents,

several of them in commercial use. He is a member of the PCCP Advisory Board.



Hermenegildo Garcia (Herme) has been a full Professor and member of the Institute of Chemical Technology at the Technical University of Valencia since 1996. He has co-authored over 300 papers and holds 10 international patents. His main current interests are in green chemistry and the use of zeolites and mesoporous materials in supramolecular photochemistry and photocatalysis.



Scheme 1 Illustration of photoinduced charge separation (electron and hole) upon illumination of a titania particle with light of energy higher than the band gap. Positive hole has sufficient oxidation potential to initiate aerobic oxidation of many organic compounds.

The above comments explain the continued interest in improving the photocatalytic efficiency of TiO_2 . To increase the photocatalytic activity of TiO_2 , particularly for visible light irradiation, two general strategies have been developed comprising either using an organic dye as photosensitizer or doping TiO_2 with metallic and non-metallic elements.^{20,22–37} The first approach (*i.e.* the use of an organic dye that absorbs visible light) has worked very well under conditions where oxygen is excluded and the degradation of the dye is minimized by efficient quenching of the dye oxidation state with an appropriate electrolyte.^{26–29,38–42} Otherwise, particularly in the presence of oxygen, the dye becomes rapidly degraded and the photocatalytic system loses its response towards visible light. The mechanism of TiO_2 dye sensitization has been determined using time resolved subnanosecond laser flash photolysis techniques.^{38–41,43,44} These studies have shown that upon light absorption, the dye in its excited electronic state injects one electron into the semiconductor conduction band. Scheme 1 illustrates a simple picture of this process.

In dye sensitization, the most relevant points are the absorption spectrum of the dye in the visible region and the energy of the electron in the excited electronic state of the dye that has to be high enough to be transferred to the semiconductor conduction band. However, electron injection of electron donor dyes in their excited state onto the TiO_2 conduction band is a quite general phenomenon since the conduction band energy of TiO_2 is not very high. In fact, TiO_2 holes are considerably much more oxidizing than the conduction band electrons are reducing.

A second chemical approach to promote photoresponse of titanium dioxide into the visible consists in doping the TiO_2 material either with metallic or non metallic elements.^{20,22–29} In this case doping introduces occupied or unoccupied orbitals in the band gap region leading to negative or positive doping, respectively. However, particularly in the case of metal doping there are contradictory reports describing either an increase or a decrease of the catalytic activity.^{13,32,34,45}

This controversy arises in part from the difficulty to establish valid comparisons about the photocatalytic activity among different solids testing different probe molecules and employing inconsistent parameters. Also the doping procedure

and the nature of the resulting material is very often not well defined and, most probably, controversial results can be obtained depending on the way in which the metal has been introduced and also depending on the final concentration of the dopant. Thus, it has often been reported that there is an optimum doping level to achieve the maximum efficiency and beyond this point a decrease in photocatalytic activity is again observed.^{30,46} Nevertheless, a consensus is starting to be achieved about the inappropriateness of metal doping as a valid solution to enhance the photocatalytic activity of TiO_2 , if not for anything else, just by the fact that the materials corrode and the dopant is leached.^{12–14,31}

More recently doping with nitrogen, carbon, sulfur and other non-metallic elements have also been reported to introduce visible light absorption of titanium dioxide.^{20,22,46–56} Asahi and co-workers were the first to show an absorption increase in the visible region upon nitrogen doping.⁴⁷ This opened the way to study titania doping with non-metallic elements.^{33,48,57} However, due to corrosion and instability of doped materials, it remains to be seen whether or not non-metallic element doping can be regarded as a general and valid approach to increase the photocatalytic efficiency of titania photocatalysts.

2. Physical methods to improve the photocatalytic response

While the above strategies to improve the photocatalytic efficiency have in common that they are based on chemical concepts which direct the modification of the chemical composition of the TiO_2 material to enhance its photocatalytic activity, in the present account we will address a different methodology to alter the photocatalytic response that is based on Physics rather than on Chemistry. In this regard, it is worth reminding that by reducing the particle size at the nanometric length scale, a point is reached behind which further decrease in the size (without altering the chemical composition) strongly influences the band gap and the position of the valence and conducting bands.^{20,58} This change in the properties with the particle dimensions is generally described as “quantum size effect” and is a well known example of operation of physical concepts in the optical properties of a semiconductor.^{59–62}

In the present review, we will describe novel methodologies to achieve the control of the photocatalytic activity of the materials by structuring the titanium oxide particles at different length scales going from subnanometers to submillimeters. Table 1 summarizes the systems studied and the length scale of the spatial structuring covered by this Perspective.

Obviously, physical and chemical concepts are not incompatible and there are a few pioneering examples in which a combination of both, doping and structuring, has been applied.^{20,57,63} For the purpose of this review the content has been organized on the length scale in which TiO_2 structuring has taken place. We will start from those reports in which TiO_2 nanoparticles of nanometric and subnanometric size have been used as photocatalysts and move towards other reports in which the spatial structuring of the photocatalyst goes into micrometric and submillimetric length scales. Although, in this

Table 1 Examples of spatial structuring of titanium oxides at various length scales

Length scale	Examples
< 1 nanometer	Titania clusters encapsulated inside zeolites
1–10 nanometers	
10 nanometers–10 micrometers	Titania nanoparticles forming periodic mesoporous powders
	Titania nanotubes
> 200 micrometers	Titania membranes
	Photonic crystals
	Photonic sponges

account we will preferentially discuss the work carried out in our group, appropriate reference to the work performed by other groups in the area has also been included to give a comprehensive view of the field. The aim of this review is to exemplify the potential and opportunities that the use of TiO₂ semiconductor with controlled size or structured in a periodic way, may have on improving the photocatalytic efficiency.

3. Photocatalytic activity of subnanometric titanium dioxide clusters

The most widely used TiO₂ photocatalyst is the Degussa P25 material.^{6,10,15,64–66} The particle size of P25 is about 25 nm and its surface area is very small (50 m² g⁻¹). A reduction of the particle size, up to a few nanometres, has the benefit of increasing the external surface area. These small particles tend to agglomerate by strong interparticle forces when the nanometric size region is reached. Further decrease of the particle size to a few nanometers reaches one point below which quantum size effects also start to operate and the band gap of the semiconductor increases, blue-shifting the absorption λ_{max} . In order to avoid the aggregation of these small subnanometric TiO₂ clusters, one methodology that has been developed consists in incorporating these TiO₂ clusters inside the rigid framework of microporous hosts. The most widely used microporous materials are large pore zeolites.^{67–70}

Zeolites are crystalline aluminosilicates in which the framework defines channels and cavities of nanometric and subnanometric dimension.^{71–74} These empty voids are normally termed micropores and are open to the exterior allowing mass transfer from a solution to the internal voids. Faujasite and zeolite beta are common large pore zeolites used for including organic and inorganic guest inside cavities^{75,76} and extra large pore tridirectional zeolite can offer new possibilities. Fig. 1 shows an illustration of the pores of Faujasite, zeolite beta and

ITQ-33. Zeolites do not absorb light in the Vis and UV region and, therefore, it is possible to irradiate guests that are incorporated inside their micropores. After all, zeolites have the same chemical composition as quartz and glasses commonly used as cells to perform photochemical reactors and optical tools.

TiO₂ can be incorporated into the micropores of zeolites.⁷⁷ There are two different strategies to form TiO₂ clusters inside zeolites. Both of them have in common the use of molecular titanium compounds having a single titanium atom that subsequently will oligomerize forming Ti–O–Ti bonds. In the first approach, vapors of TiCl₃ or TiCl₄ are absorbed into zeolite totally or partially dehydrated and in the second step hydrolysis and oligomerization to form TiO₂ clusters is promoted by thermal treatment in the presence of moisture.^{69,70,78} Depending on the level of dehydration of zeolite, the formation of TiO₂ aggregates can take place predominantly on the exterior (when water fills the pores during the titanium absorption) or in the interior (when titanium halides are adsorbed in the interior of the micropores before hydrolysis) of the zeolite micropores. The main problem of TiCl₃ is that it is an explosive and pyrophoric compound, while both TiCl₃ and TiCl₄ form highly corrosive HCl vapors upon hydrolysis.^{79–81} These harsh acid conditions can damage to some extent the zeolite structure particularly producing a partial loss in crystallinity.

Alternatively, TiO₂ clusters can be formed inside the zeolite from the aqueous phase by ion exchanging of Na⁺ (the counter cation normally present in synthetic zeolites) by (Ti=O)²⁺ titanyl salts.^{82,83} These salts are commercially available, they are non-corrosive and the ion-exchange process can be carried out in water. Scheme 2 illustrates the two different methodologies used to introduce TiO₂ inside the zeolite.

After ion exchange, hydrolysis and oligomerization of titanyls (Ti=O²⁺) can be carried out simply by treatment of the Ti=O²⁺ containing zeolite at mild temperatures of about 150 °C. The main drawback of titanyl is the difficulty in controlling the amount of incorporated titanium, particularly for low loadings.

By using vapor phase adsorption of TiCl₄, Schulz-Ekloff and co-workers have prepared titanium oxide-containing zeolite in which UV/Vis spectroscopic characterization suggests that at low loadings isolated titanium atoms mono-, bi- or tripodally anchored to the zeolite framework are formed.⁶⁷ Higher loading can lead to aggregates in which Ti–O–Ti bonds are present. It has been proposed that isolated titanium atoms

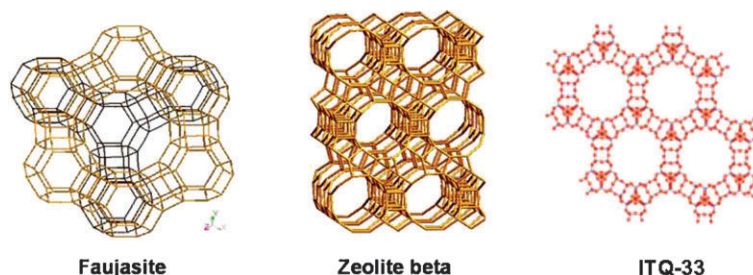
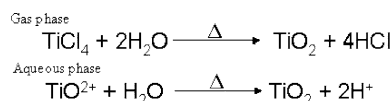


Fig. 1 Structure of zeolites Faujasite, beta and ITQ-33 in which the micropores are defined by the framework.



Scheme 2 Alternative procedures to form subnanometric TiO₂ clusters inside the zeolite micropores based on adsorption of compounds containing a single titanium atom.

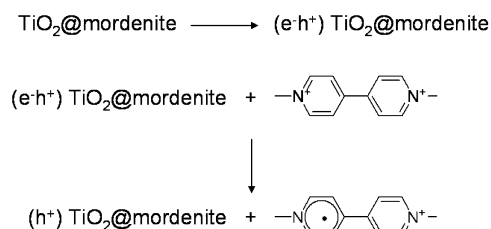
in a Si–O–Ti configuration have an absorption λ_{max} at around 220 nm while clusters with Ti–O–Ti bonds absorb at in the UV spectra at 240 and higher wavelength.⁶⁷ Identical spectroscopic criterion has been applied to crystalline titanosilicates that are widely used as oxidation catalysts.^{84–86}

In these zeolite samples containing monoatomic Ti^{IV}, easy formation of Ti^{III} by reduction of Ti^{IV} ions can occur and this can simply be detected by a characteristic Ti^{III} absorption band at around 630 nm that is responsible for the blue tint of the powdered sample.^{69,87}

On the other hand, Thomas *et al.* have prepared clusters of TiO₂ in mordenite using water soluble titanil salts.^{82,83} Incorporation of titanium in zeolite by using of Ti=O²⁺ is an ion exchange process in water that may require consecutive cycles using increasing Ti=O²⁺ concentrations in order to achieve high TiO₂ loadings. TiO₂ clusters incorporated inside the zeolite voids exhibit photocatalytic activity for the reduction of methyl viologen.⁸² Thus, upon TiO₂@mordenite irradiation, the corresponding viologen radical cation is generated and can be detected spectroscopically (Scheme 3).

Scaiano and Garcia using the same procedure described by Thomas, have prepared a large series of TiO₂ containing zeolites in which the zeolite chemical structure and the titanium loading were varied.^{88,89} High resolution transmission microscopy as well as XPS (taken as analysis of the external surface of the zeolite particles) and other characterization techniques established that in most of the samples, titanium was incorporated inside the zeolite micropores with only minor occasional isolated TiO₂ nanoparticles detected outside the zeolite particles.⁸⁸ By Raman spectroscopy (Fig. 2) it was determined that the zeolite encapsulated TiO₂ clusters are present as a mixture of anatase-like and rutile-like structures. Raman is a powerful spectroscopic technique that together with X-ray diffraction serves to distinguish the anatase or rutile phases of TiO₂.

By means of diffuse reflectance UV/Vis spectroscopy (Fig. 3), it was observed that the TiO₂ clusters incorporated inside zeolites have an onset of the absorption band significantly blue shifted as compared to conventional P25 TiO₂ nanoparticles.⁸⁸ This blue shift becomes more remarkable when the titanium loading in the zeolite decreases and is



Scheme 3 Generation of the methyl viologen radical cation upon irradiation of a zeolite containing TiO₂ clusters (based on ref. 82).

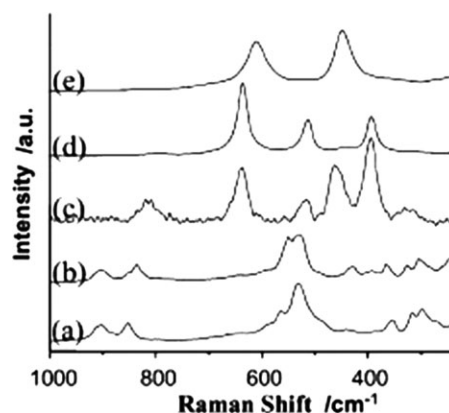


Fig. 2 Raman spectra of (a) TiO₂⁺ in water; (b) TiO₂⁺@Y zeolite; (c) sample b after heating at 150 °C for 1 h; (d) TiO₂ in anatase phase; (e) TiO₂ in rutile phase.

considered a reflection of the operation of quantum size effects. Also remarkable is that the slope of the absorption band is more vertical for highly loaded samples suggesting that in these cases the samples have a more homogeneous size distribution of encapsulated titanium clusters, probably corresponding to the volume of the zeolite cavity.

Photoluminescence is a hallmark of small nanoparticles that is lost for TiO₂ above 20 nm. In this regard it is interesting that, in accordance with the subnanometric cluster size of the TiO₂ clusters incorporated inside zeolites, TiO₂@zeolite exhibits photoluminescence that is not observed in P25.^{89,90}

These samples of zeolite encapsulated TiO₂ show photocatalytic activity for the photooxidation of thianthrene (Table 2).⁸⁸ This heterocyclic compound can be considered a model for sulfur-containing aromatic compounds present in fuels and heavy oil fractions that are responsible for the formation of SO_x during combustion processes.^{91,92} There is a research line to carry out the oxidation of these sulfur heterocycles to more polar water-soluble sulfoxides and sulfones, not only by regular catalytic oxidation but also by photooxidation.⁹³ Importantly, Table 2 shows that the photocatalytic activity of zeolite encapsulated TiO₂ can be higher than P25 standard.⁸⁸ This photocatalytic enhancement has been ascribed mainly to the favorable adsorption of

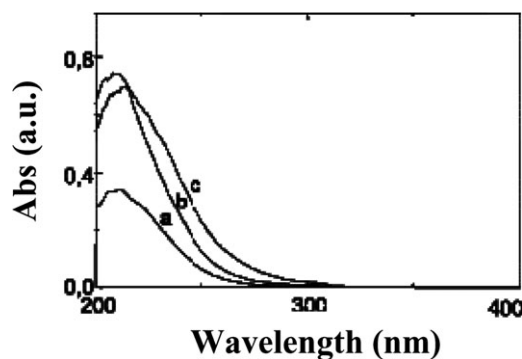
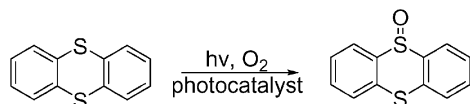


Fig. 3 Diffuse reflectance optical spectrum of a series of three zeolite Y samples containing increasing titanium loadings (titanium concentration increase in the order a < b < c).

Table 2 Results of the photocatalyzed TH oxygenation upon 254 nm UV lamp after 1 h irradiation (data taken from ref. 88)

Photocatalyst	Yield of TH = O%
NaY	2
TiO ₂ @Y (first exchange)	22
TiO ₂ @Mordenite (first exchange)	21
P25 TiO ₂	4

thianthrene (TH) inside the zeolite micropores.



In the previous examples thianthrene, being a relatively small molecule, can diffuse inside the zeolite micropores and become oxidized in the photocatalytic process. Incorporation of TiO₂ inside a restricted reaction cavity offers in addition the possibility to increase the photoactivity for certain substrates avoiding, at the same time, the degradation of the molecules that do not enter into the zeolite internal pores. For example, the same TiO₂@zeolite samples that were able to perform the photocatalytic oxidation of TH were remarkably inefficient for the inactivation of horseradish peroxidase (HRP), an enzyme that is able to decompose hydrogen peroxide. Fig. 4 shows the HRP inactivation upon irradiation of solutions of this enzyme in the presence of a series of titanium dioxide photocatalysts including P25 and TiO₂@Y.

As can be seen in Fig. 4, TiO₂ inactivates to a considerable extent the ability of HRP to oxidize 2,2'-azinobis(3-ethylbenzothiazoline-6-sulfonic acid), while due to the large size of this macromolecule, TiO₂@zeolite produces only a minor damage of the enzyme, the catalytic activity of the native enzyme being largely preserved when this enzyme is irradiated in the presence of TiO₂@zeolite.

This selectivity of TiO₂@zeolite to attack small molecules can be highly beneficial in those cases in which the photoactivity of TiO₂ plays an adverse effect. This is the case of sun screens for topical use in cosmetics.⁹⁴ For this application in which the titanium dioxide nanoparticles are going to be exposed to the solar light, it is necessary to ensure that TiO₂ is avoiding any photocatalytic activity against human skin.⁹⁴

Using crystalline titanosilicate having TiO wires, Zecchina and co-workers have coined the term “inverse shape-selective” photocatalysis to reflect the preferential photocatalytic degradation of large phenols with respect to smaller phenols that can access to the zeolite interior.⁹⁵ In contrast to what is seen in TiO₂@zeolite (photocatalysis of adsorbed molecules) in the case of crystalline titanosilicate of the ETS family only Ti–O wires externally placed in the crystals are photocatalytically active.⁹⁵

Following the pioneering lead of Mallouk, who wanted to develop zeolite-based photocatalyst for water splitting,^{96–98} Bossmann and co-workers were the first to report a multi component system containing Ru(bpy)₃²⁺ and TiO₂ simultaneously incorporated inside zeolite Y.⁷⁸ Due to the importance of dye sensitized solar cells in which photoexcitation of polypyridyl ruthenium complexes lead to a fast electron injection

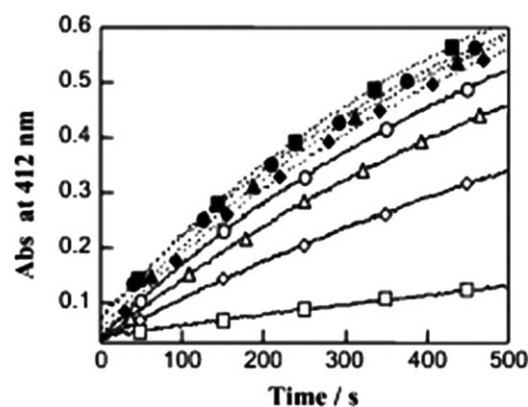
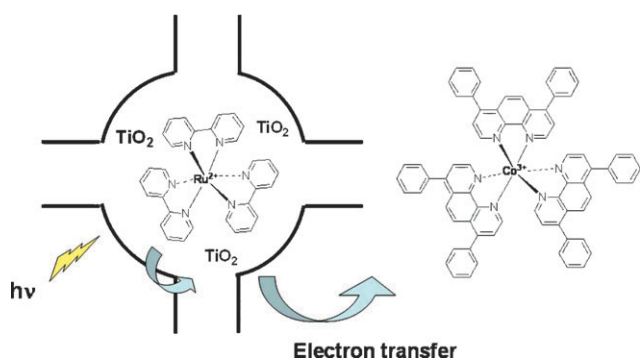


Fig. 4 Enzymatic activity of HRP (measured through its ability to catalyze the oxidation of 2,2'-azinobis(3-ethylbenzothiazoline-6-sulfonic acid) diammonium salt that is monitored by the absorbance at 412 nm) as a function of the irradiation time in the presence of a series of photocatalysts. ● and ○ HRP; ▲ and △ HRP + TiO₂@Y; ◆ and ◇ HRP + TiO₂@MOR; ■ and □ HRP + TiO₂ anatase. Black symbols non-irradiated and open symbols irradiated samples.

into the TiO₂ conduction band, the Ru(bpy)₃²⁺/TiO₂ couple has properties worth exploring in very different environments.

In the case of zeolite-encapsulated TiO₂ there are several possible topologies, including those in which the large Ru(bpy)₃²⁺ is size excluded from the zeolite interior and adsorbed on the zeolite external surface, while the semiconductor oxide is located in the internal voids.⁹⁹ In the examples reported by Bossmann *et al.*, Ru(bpy)₃²⁺ (about 1.2 nm diameter) is accommodated inside the cavities of zeolite Y (spherical cages of about 1.3 nm) but it becomes immobilized because this metallic complex cannot diffuse through the smaller cavity windows (0.74 nm). This internally entrapped Ru(bpy)₃²⁺@zeolite can be easily prepared by a ship-in-a-bottle synthesis starting from Ru(NH₃)₄³⁺@zeolite and adding 2,2'-bipyridine.^{100–102} When a sample of Ru(bpy)₃²⁺@zeolite is modified by TiO₂, the system contains immobilized Ru(bpy)₃²⁺ ions in close proximity to subnanometric TiO₂ cluster co-incorporated in the same or neighbouring cavity of the material. Using the photoinduced electron transfer between zeolite entrapped Ru(bpy)₃²⁺ and size-excluded Co(dpphen)₃³⁺ (dpphen = 4,7-diphenyl-1,10-phenanthroline) in the exterior of zeolite particles, Bossmann observed that the relative efficiency of the quenching of internal Ru(bpy)₃²⁺ by external Co(dpphen)₃³⁺ increases along the titanium content into the zeolite (Scheme 4).⁷⁸ This observation indicates that TiO₂ nanoparticles are acting as electron relays, promoting the electron transport from photoexcited Ru(bpy)₃²⁺ located inside the zeolite to external Co(dpphen)₃³⁺. The bicomponent [Ru(bpy)₃²⁺/TiO₂@zeolite] photocatalyst shows a high activity for the degradation of 2,4-xylydine considered as a model pollutant of aromatic amines.¹⁰³ An analogous system also developed by this group and tested for the photo-Fenton degradation of 2,4-xylydine has been [Fe(bpy)₃²⁺/TiO₂@zeolite].¹⁰⁴ Given the lack of reusable photo-Fenton catalysts, this material shows promise as a recoverable photo-Fenton catalyst.

Similar samples of Ru(bpy)₃²⁺/TiO₂@Zeolite Y have been studied by Scaiano and Garcia by means of fluorescence,



Scheme 4 Pictorial illustration of photoinduced electron transfer between encapsulated $\text{Ru}(\text{bpy})_3^{2+}$ and external $\text{Co}(\text{dphen})_3^{3+}$ favored by small TiO_2 clusters acting as electron relays (based on ref. 78).

steady-state and time-resolved, as well as laser flash photolysis.¹⁰⁵ It was observed that this sample exhibits reduced emission and shorter life time from $\text{Ru}(\text{bpy})_3^{2+}$ excited state triplet and it undergoes prompt photoinduced charge separation compared to analogous $\text{Ru}(\text{bpy})_3^{2+}$ @Y materials lacking TiO_2 . This was taken as evidence of the interaction between $\text{Ru}(\text{bpy})_3^{2+}$ in its excited state and co-adsorbed TiO_2 clusters. Similarly, a Y zeolite containing 2,4,6-triphenylpyrylium (TP^+) and TiO_2 has been prepared.¹⁰⁵ Fig. 5 shows a molecular model of TP^+ encapsulated within the cavities of zeolite Y. Spectroscopic characterization using time resolved photoluminescence and laser flash photolysis also revealed an interaction between the light-absorbing dye in its excited state and TiO_2 clusters. Photocatalytic experiments using HRP deactivation in buffered aqueous solution showed that deactivation of HRP is considerably more important for bifunctional ($\text{Ru}(\text{bpy})_3^{2+}/\text{TiO}_2$ or TP^+/TiO_2) systems encapsulated in zeolites than the photocatalytic activity of each of the individual components inside the zeolite.¹⁰⁵

A more complex system in line with those previously described is the one containing $\text{Ru}(\text{bpy})_3^{2+}/\text{TiO}_2/\text{TP}^+$ inside Y zeolite (Scheme 5).¹⁰⁶

This is a three component system in which an electron donor [$\text{Ru}(\text{bpy})_3^{2+}$] and an electron acceptor (TP^+) are simultaneously immobilized within the zeolite cavities and interposed by TiO_2 acting as an electron relay. In this case using fluorescence to monitor the interaction between $\text{Ru}(\text{bpy})_3^{2+}$

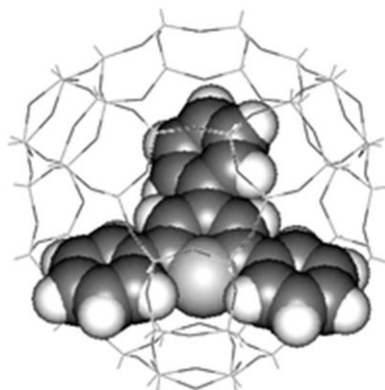
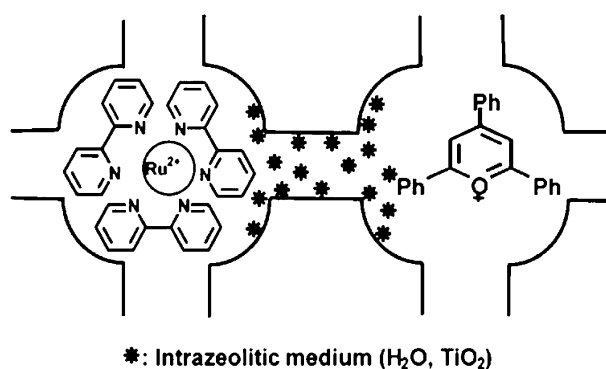


Fig. 5 Molecular model of TP^+ cation occupying the cavities of zeolite Y.

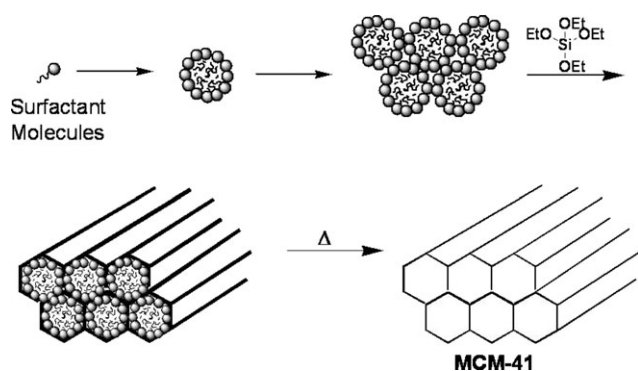


Scheme 5 Illustration of zeolite Y encapsulated $\text{Ru}(\text{bpy})_3^{2+}$ complex and TP^+ cation in neighbouring supercages. The intrazeolite space between the electron donor [$\text{Ru}(\text{bpy})_3^{2+}$] and the electron acceptor (TP^+) can be occupied by TiO_2 or absorbed water (based on ref. 106).

and TP^+ , it has been observed that the TiO_2 clusters interposed between $\text{Ru}(\text{bpy})_3^{2+}$ and TP^+ disfavours the interaction between the donor and the acceptor, restoring the $\text{Ru}(\text{bpy})_3^{2+}$ emission to 90% of the original value in the absence of TP^+ quenchers. Experimentally, the photoinduced electron transfer between excited $\text{Ru}(\text{bpy})_3^{2+}$ and a good electron acceptor as TP^+ is more efficient when no TiO_2 is located between these two termini. This has been interpreted considering that the higher LUMO energy for encapsulated TiO_2 clusters, in which quantum size effects increase the band gap as compared to TiO_2 nanoparticles of 25 nm, disfavours the ability of TiO_2 to act as a semiconductor. Thus, electron injection is energetically less favourable for encapsulated TiO_2 clusters than for P25 and the injected electrons less mobile and more trapped than in conventional large TiO_2 particles. Therefore, encapsulated TiO_2 behaves, in this case, more as insulator than as an electron relay. Overall the previous studies show the ease of preparation of encapsulated TiO_2 clusters inside micropore hosts and the advantages in terms of high efficiency and size control of the photocatalytic activity. In this regard, Anpo and coworkers have made substantial contributions towards the application of zeolite-encapsulated TiO_2 clusters as photocatalysts for NO_x and CO_2 fixation.^{58,107–116} Overall, in addition to the examples of increased photocatalytic activity, the observed harnessing of the TiO_2 photocatalytic activity and the introduction of some kind of substrate selectivity is a subject that still requires considerable attention to be exploited in full.

4. Nanometric structuring: mesoporous titanium dioxide as photocatalysts

The original report from Mobil researchers describing the synthesis of structured mesoporous silicas using the surfactant template methodology constituted a breakthrough in material chemistry in the 90s.^{117–119} Surfactant molecules, in concentrations above the critical micellar concentration (cmc) undergo in aqueous media spontaneous self assembly forming micelles. Further increases in surfactant concentration leads to rods in which the aqueous colloidal surfactant solution can be considered as a liquid crystal phase. Concomitant hydrolysis, oligomerization and polycondensation of soluble silica



Scheme 6 General formation mechanism of a MCM-41 material.

precursors occur at the water–surfactant rod interphase, the silica polymer acquiring the shape of the rods. Initially the surfactant rods are not rigid and fairly independent of each other, but as the silica phase densifies and grows the rods bind together in a close packing configuration. The resulting solid after considerable oligomerization/condensation of the silicon precursor and removal of the template is a material with extraordinary periodicity formed by channels of strictly regular dimensions in the nanometric scale (from 2 to 10 nm). Thus, mesoporous silicas constituted a logical extension of the zeolite materials. Scheme 6 illustrates the mechanism of formation of MCM-41 mesoporous material.

The regularity of the channels and walls in MCM-41 is so remarkable that the material shows X-ray ordering at long distances, even though the material does not have a short distance order. The terms “periodic” or “structured” have been used to denote this type of solid that are amorphous at the subnanometric scale but exhibit order in the nanometric length scale. Fig. 6 shows transmission electron microscopy images in which side and frontal views of the channels are presented. The consequence of mesoporosity is that these materials rank at the top of the list of the large surface area solids with values for specific internal surface and pore volume as high as $1000 \text{ m}^2 \text{ g}^{-1}$ and 1 ml g^{-1} . For comparison common values of surface area and volume in zeolite can be $400 \text{ m}^2 \text{ g}^{-1}$ and 0.3 ml g^{-1} .

Shortly after the original report from Mobil, there was an interest in expanding the results initially obtained for silica and silico-titanate to most of the transition metal oxides. This subject has been reviewed several times.^{120–122} Titania is an obvious example of metal oxide that can benefit from being prepared as a periodic mesoporous solid. For photocatalytic applications, the large surface area and pore volume characteristics of mesoporous materials will play a positive role in

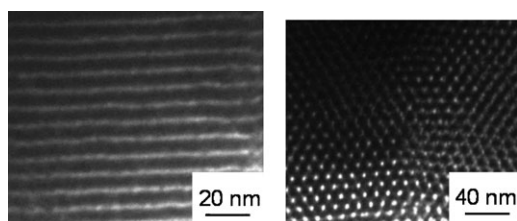


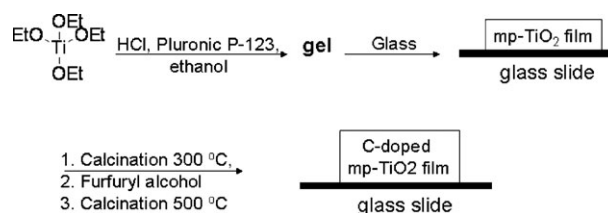
Fig. 6 TEM images showing a parallel (left) and perpendicular (right) view of the channels in MCM-41 material.

photocatalysis. Even more importantly and less evident, structuring can affect the length of the charge migration in the charge separate state.

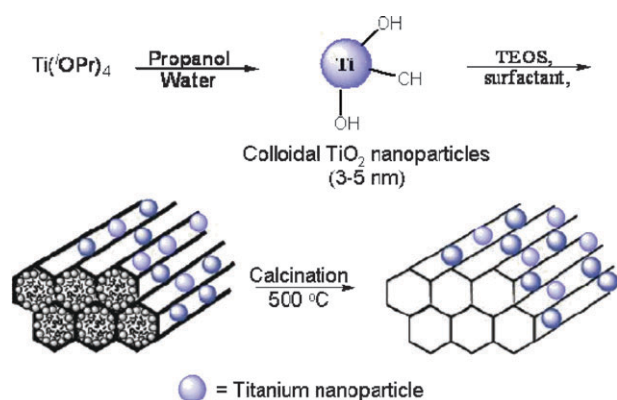
One of the advantages of sol–gel synthesis of mesoporous materials is the possibility to form uniform films on a substrate. Using the method studied in detail by Sanchez *et al.*,^{123,124} a uniform film of mesoporous titania on glass substrate can be obtained dipping the glass slide into an acidic solution of titanium alcoxide in ethanol. Immediately after dipping the glass, the surfactant concentration is lower than the cmc, but as the glass is removed from the solution and ethanol evaporates, the cmc point is reached and the surfactant starts to template the formation of thin layers of a mesoporous titanium oxide. The key point is to control carefully the rate of solvent evaporation that has to be sufficiently slow to allow the templation and oligomerization of the titanium oxide around the self assembled micelles created by the surfactant in its liquid crystal state. Applying the above methodology, highly structured materials constituted by anatase nanoparticles (5–10 nm) ordered forming a mesoporous film (mp-TiO₂) perpendicular to the glass slide have been prepared by Stucky *et al.*¹²⁵ The as-synthesized mp-TiO₂ material is initially structured in the 5–100 nm length scale forming mesopores, but the walls are formed by an amorphous TiO₂ phase. Calcination of the material produces crystallization of the as-synthesized amorphous titanium dioxide into anatase phase without destroying the mesoporous ordering of the film. Careful control of the calcination temperature (< 550 °C) is crucial to avoid the formation of the rutile phase that, as expected in view of its lower activity, is significantly less photocatalytic active than the material constituted by the anatase phase.

Films of structured mesoporous mp-TiO₂ anatase materials filled with furfuryl alcohol as the source of polymeric carbon have been used as photoanodes for water photolysis using a xenon lamp.¹²⁶ Scheme 7 presents the route followed for the preparation of these carbon containing mp-TiO₂ photocatalysts. The maximum efficiency of photon-to-hydrogen conversion of 2.5% was obtained with carbon doped titanium dioxide and it was more than four times higher than analogous mesoporous TiO₂ films prepared without furfuryl alcohol.¹²⁶

Following an analogous methodology, but impregnating the ordered mp-TiO₂ anatase films with silver instead of carbon, the resulting films have been used as photocatalysts for the oxidative degradation of stearic acid.¹²⁷ A control experiment comparing the activity with analogous mp-TiO₂ films without silver nanoparticles has shown that the metal particles notably increase the initial degradation rate. However at long



Scheme 7 Preparation of a mesoporous anatase film filled on conductive carbon that has been used as photoanode for the production of hydrogen (based on ref. 126).



Scheme 8 Synthetic procedure of mesoporous titania/silica materials in which colloidal titania nanoparticles (3–5 nm) have been used as building blocks (taken from ref. 128).

irradiation times the presence of silver seems to be detrimental for the catalytic activity of the materials.¹²⁷ As one of the possible reasons to explain this lower photocatalytic activity upon use, it has been proposed that poisoning or deactivation of Ag nanoparticles by degradation intermediates may take place. The previous two examples in which the channels of mesoporous titania have been used to host conductive carbon and silver nanoparticles, both species cooperating in the photocatalytic activity, illustrates the vast potential of these materials with respect to non-porous conventional anatase nanoparticles. Encapsulation of guests inside mesoporous TiO_2 should allow the use of host/guest supramolecular chemistry to increase the photocatalytic activity of TiO_2 .

A different synthetic strategy in which preformed TiO_2 nanoparticles (3–5 nm) are used as building blocks in combination with variable proportions of tetraethyl orthosilicate (TEOS) has also been used to form structured mesoporous materials.¹²⁸ The role of TEOS is to bind the titanium dioxide nanoparticles through Si–O–Ti bonds in such a way that, on the one hand, the presence of TEOS holds the TiO_2 nanoparticles forming a rigid matrix, while on the other hand TEOS favors the action of the surfactant templating the material. Scheme 8 shows the procedure followed to prepare these mesoporous materials obtained from preformed TiO_2 nanoparticle building blocks.

As surfactants to template the synthesis of mp- TiO_2 by assembly of TiO_2 nanoparticles either CTABr or Pluronic-123 were used.¹²⁸ After calcination, TEM images and powder XRD showed that the materials have mesoporous ordering. Raman spectra also indicate that the predominant TiO_2 phase is anatase. Fig. 7 shows selected TEM images corresponding to these mesostructured mp- TiO_2 titania photocatalysts containing variable proportions of silica.

In contrast to some other reports in which mixed Ti/Si oxides exhibited a band gap energy, energy levels as well as photocatalytic activity strongly influenced by the composition of the mixed oxide,¹²⁹ the previous mp- TiO_2 materials have separate and independent TiO_2 and SiO_2 domains covalently bonded through a few Ti–O–Si linkage at the interphase. One of these domains is formed by anatase nanoparticles for which silica is not interfering with the band gap levels because it is present as a separate phase.

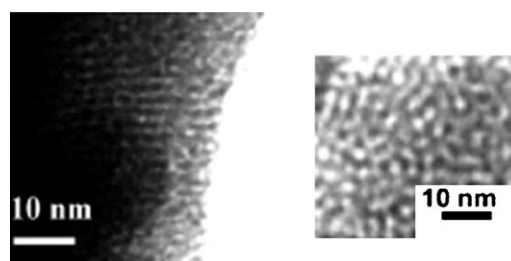


Fig. 7 Transmission electron microscopy images of side (left) and front (right) views of mp- TiO_2 materials obtained using colloidal TiO_2 nanoparticles as building blocks (taken from ref. 128).

The photocatalytic activity of mp- TiO_2 has been studied for the degradation of phenol in water solutions.¹²⁸ It was observed that for those structured mesoporous TiO_2 samples having low titanium content, the turnover frequency (TOF, mol of degraded phenol \times mol of titania⁻¹ \times h⁻¹) value can be four times higher than the standard P25. However, as the titanium content of the material increases (mp- TiO_2 with 99% TiO_2 and 1% TEOS), the TOF for phenol degradation decreases and the material mp- TiO_2 with very low silicon content and hexagonal ordering has a catalytic activity measured by TOF about 4 times lower than P25. Since TOF measures the activity per each titanium atom, the influence of the titanium content in the TOF value has been interpreted as reflecting the beneficial influence of accessibility and isolation of the TiO_2 domains on the intrinsic activity of titanium atoms.

An interesting application of photocatalysis, consists in pursuing the synthesis of organic compounds rather than the degradation and destruction of them. Albin has coined the term “positive photocatalysis” to describe this aspect of photocatalysis.^{130,131} In this regard, photooxidation of alkanes to ketones is one of the most important reactions that can be performed using titanium dioxide.¹³² One example of alkane photooxidation that could have a large economical impact is the conversion of cyclohexane into cyclohexanol and cyclohexanone.^{132–135} The key point in this reaction is to reach high selectivity to cyclohexanone at high conversions. Although poorly understood, it has been found that the nature and structuring of the mp- TiO_2 photocatalyst has a remarkable influence on the selectivity towards cyclohexanone.¹³⁶ Thus, structured mp- TiO_2 exhibits at irradiation wavelength longer than 290 nm a remarkable higher selectivity towards the formation of cyclohexanone than P25.¹³⁶ This difference in product selectivity between the mesoporous and non-mesoporous titania disappears when the irradiation is carried out with filtering short wavelength light from the excitation irradiation. Table 3 shows relevant photocatalytic data for the photooxygenation of cyclohexane in which the higher selectivity towards formation of cyclohexanone of mp- TiO_2 with respect to P25 TiO_2 at the same conversion using short wavelength irradiation can be seen.

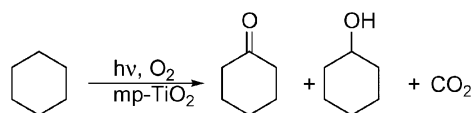


Table 3 Selectivity of cyclohexane oxygenation using two titania photocatalysts as a function of the excitation light (data taken from ref. 136)

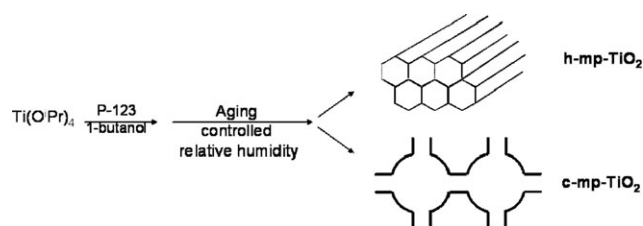
λ excitation/nm and light intensity/W cm ⁻²	Photocatalyst	Alcohol (%)	Ketone (%)	CO ₂ × 1/6 (%)
> 290 2.8 × 10 ⁻²	mpTiO ₂	4	89	7
> 290 2.8 × 10 ⁻²	P-25 TiO ₂	11	81	8
> 350 7.8 × 10 ⁻³	mpTiO ₂	3	90	7
> 350 7.8 × 10 ⁻³	P-25 TiO ₂	1	90	9

It has been proposed that the difference in product selectivity arises from the better absorption of peroxy radicals on the mesoporous surface that favors its consecutive reduction by trapped electrons.¹³² Compared to amorphous non-porous titania, the mesoporous photocatalyst must adsorb the peroxy radical stronger and does not desorb this species into the solution (Scheme 9).

Ozin and coworkers have also prepared films of mesoporous mp-TiO₂ on glass.¹³⁷ Pluronic-123 (P-123) was used as a structure directing agent and 1-butanol as the solvent. By careful control of the preparation conditions, particularly temperature and relative humidity, two mesoporous mp-TiO₂ films having 2D hexagonal (h-mp-TiO₂) and a 3D cubic (c-mp-TiO₂) structure were obtained (Scheme 10).

The channels of h-mp-TiO₂ run perpendicularly to the substrate and therefore they should be accessible for substrate incorporation. After preparation, the films were submitted to three different annealing temperatures up to 459 °C, crystallinity increasing with the annealing temperature. Thus, all the h-mp-TiO₂ samples consisted of variable proportions of anatase nanoparticles in a matrix of amorphous titania.

The photocatalytic activity of these films was tested for the degradation of methylene blue (MB), the photocatalytic reaction being followed by optical spectroscopy.¹³⁷ For the photocatalytic degradation in dry conditions, a constant surface coverage of 0.6 was selected. A summary of the results is shown in Table 4. It was observed that the photocatalytic activity of mesoporous materials annealed at 450 °C is over 1.5 times higher than the analogous film constituted by 100% anatase prepared in the absence of P-123 (nc-TiO₂ in Table 4). It was concluded from these solid state experiments that the degree of crystallinity was the main factor governing the photocatalytic activity and that the morphology of the mesopores does not play any role. This conclusion is based on experiments in which all the samples have been studied at the same surface coverage and, therefore, mesoporous samples with higher surface area than non-porous titania contain a higher loading of MB.



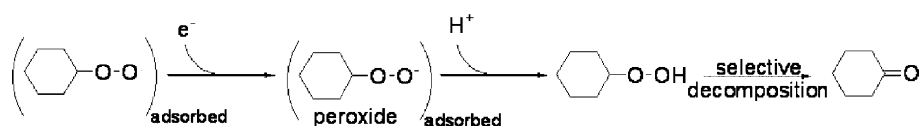
Scheme 10 Preparation of films of 2D and 3D structured titania photocatalyst (based on ref. 137).

Table 4 Results of the photocatalytic decoloration of MB adsorbed on a series of mesoporous (hexagonal, h, or cubic, c) and non-porous (nanocrystalline, nc) titania samples at the same surface coverage (data taken from ref. 137)

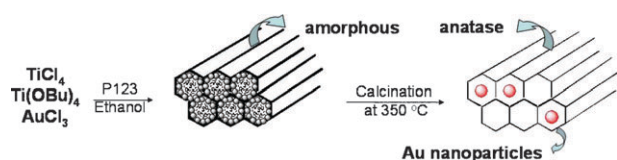
	Annealing temperature/°C	Crystallinity of anatase (%)	Apparent constant rate solid state/k min ⁻¹
h-meso-TiO ₂	400	69	0.07
h-meso-TiO ₂	450	86	0.10
c-meso-TiO ₂	400	84	0.09
c-meso-TiO ₂	450	98	0.13
nc-TiO ₂	450	100	0.07

In contrast to this measurement in the absence of solvent, the kinetics of the degradation of 5 μM MB aqueous solution is significantly more complex due to the combination of many factors including titania crystallinity, surface area, diffusion coefficients, adsorption, *etc.*¹³⁷ Thus, for the degradation of aqueous solutions it was found that annealing at 400 °C provides the material with the optimum activity. Overall the above results establish that the porous structure affects positively the photocatalytic activity compared to conventional non-porous titania. It has to be noted, however, that the degradation of MB using titania photocatalyst constitutes a specific mechanistic case in which light initiating photodegradation is absorbed by the dye rather than by the titania. For many other cases, the substrate does not absorb light and it has to be titania which should be excited by direct light absorption.

A further development of mesoporous titania as photocatalyst has been reported by Li, Lu and coworkers.¹³⁸ These authors have prepared a photocatalyst constituted by mesoporous titania embedding gold nanoparticles (Au/mp-TiO₂). Its preparation requires P-123 as structure directing agent, a mixture of TiCl₄ and Ti(OBu)₄ and AuCl₃ as the source of gold using ethanol as solvent. The gel is cast on a Petri dish to form a thin layer that is subsequently aged at 100 °C to form a homogeneous mesostructured nanocomposite. Calcination at 350 °C in air removes the template while inducing crystallization of TiO₂ and formation of gold nanoparticles. Scheme 11 presents the procedure followed to obtain this mesoporous titania containing gold.



Scheme 9 Proposed mechanism to justify the higher selectivity towards cyclohexanone when radicals remain adsorbed on the TiO₂ surface.



Scheme 11 Preparation of Au/mp-TiO₂ (based on ref. 138).

This Au/mp-TiO₂ material was tested for the photocatalytic degradation of phenol and for the reduction of chromium(vi).¹³⁸ The results show that the presence of gold nanoparticles at 0.5 wt% increase the photocatalytic activity about 1.5 and 3.5 times for phenol oxidation and chromium(vi) reduction, respectively, as compared to analogous mesoporous titania material lacking gold. It would also be of interest to have a valid comparison of the photocatalytic activity of these materials with that of standard P25.

5. From nanometric to micrometric structuring: titania nanotubes as photocatalyst

Titania materials of 1D dimensionality such as nanotubes, nanofibers and nanowires have also attracted attention for their use in photocatalysis.^{139–142} In particular titania nanotubes being tens to hundreds of nanometers in diameter and micrometric length have been the subject of intensive study. Titania nanotubes have a relatively high surface area compared to non-porous titania and time-resolved diffuse-reflectance spectroscopy has shown that charge recombination is disfavored by the tubular morphology of the titania. These titania nanotubes (NT-TiO₂) can be conveniently obtained starting from titania nanoparticles as, for instance P-25, that are digested under strong basic conditions in an autoclave at about 150 °C for several hours.¹⁴³ Annealing of these NT-TiO₂ at 400 °C for 3 h renders nanotubes that are composed 100% by anatase. Laser flash photolysis of the NT-TiO₂ compared with conventional titania nanoparticles has allowed to estimate apparent quantum yield of charge separation (ϕ_{cs}). Table 5 lists some of the ϕ_{cs} values measured for NT-TiO₂ compared with different conventional spherical nanoparticles powders.

Notably the half life of the photogenerated hole (h^+) is significantly longer for NT-TiO₂ as compared to nanoparticles.¹⁴³ Furthermore when 4-(methylthio)phenylmethanol (MTPM) was added to the slurry as a hole quencher, the characteristic absorption band of the MTPM⁺ radical cation (around 550 nm) was observed.¹⁴³ This MTPM⁺ adsorbed on NT-TiO₂ exhibits remarkably longer half-lives compared to the situation in which MTPM⁺ is adsorbed on nanoparticles. This has been attributed to a longer diffusion length of the charge carriers (>200 nm) as a consequence of the low dimensionality of the nanotubes. Analogously, a higher diffusion length of charge carriers has also been claimed by Yanagida *et al.* to justify the higher efficiency of electron transport in NT-TiO₂ electrodes compared to analogous electrodes prepared with nanoparticles.⁴² Fig. 8 illustrates the proposal to justify the long lifetime of charge separation in titania nanotubes.

Table 5 Surface area and photophysical data obtained by laser flash photolysis of NT-TiO₂ and other TiO₂ materials

TiO ₂ ^a	BET surface area/m ² g ⁻¹	ϕ_{cs}	$\tau_{1/2}/\mu s$
NT-TiO ₂ -400	225	2.0	3.5 + 0.4
Standard TiO ₂ -1	300	7.1	0.6 + 0.2
Standard TiO ₂ -2	50	4.8	1.0 + 0.2
Standard TiO ₂ -3	10	1.6	0.7 + 0.2

^a Standard TiO₂ corresponding to commercial samples of spherical shaped nanoparticles.

The consequence of the low dimensionality of NT-TiO₂ can also be revealed by steady-state diffuse-reflectance spectroscopy after UV irradiation (365 nm) of a suspension of nanotubes in aerated acetonitrile containing MPTM in which the photogeneration of an increase concentration of trapped electrons is clearly observed (Scheme 12). These trapped electrons can serve to degrade CCl₄. Importantly, none of the photocatalysts constituted by nanoparticulate powder exhibit a similar behavior.¹⁴³ Thus, these studies nicely exemplify the advantage of having TiO₂ spatially organized as nanotubes instead of independent nanoparticles.

Compared to the use of independent TiO₂ nanotubes, it is even more interesting to have an ordered array of these nanotubes. Thus, a surface of NT-TiO₂ (0.8 cm²) in which they are ordered perpendicularly to the substrate has been obtained by anodization of a titanium foil in an electrolyte consisting in 1 M NH₄H₂PO₄ + 0.5 wt% NH₄F and applying a voltage of 15 V.¹⁴⁴ The surface of these TiO₂ nanotubes (70 nm diameter and 20 nm walls thickness) could be doped with carbon by thermal treatment between 500 and 800 °C under controlled CO gas flow.¹⁴⁴ The resulting carbon doped NT-TiO₂ exhibits higher photocurrent density and more efficient photocatalytic water splitting under visible light illumination ($\lambda > 420$ nm) than undoped NT-TiO₂ and a total photocurrent more than 20 times higher than that of a film of P25 nanoparticles. Thus, these measurements parallel to those that have been made with films of carbon-doped mp-TiO₂ as photoanodes can cause water splitting.

Analogously, Schmuki and coworkers have prepared large surfaces of ordered NT-TiO₂ of various lengths from 0.5 to 4.5 μm .¹⁴⁵ The deepest films have tubes of 45 nm diameter, while a common diameter for most of the films is 100 nm. After preparation by anodization, the nanotubular films were annealed at 450 °C, a calcination temperature that was found

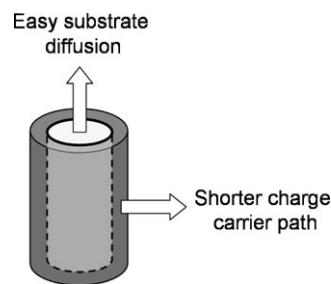
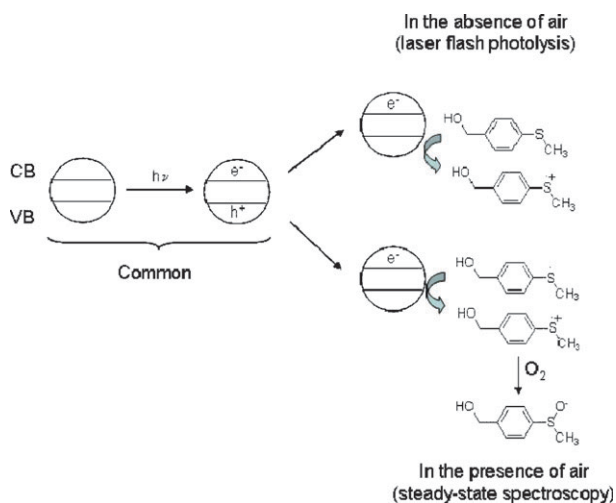


Fig. 8 Pictorial representation of the advantages derived from the use of titania nanotubes. The aspect ratio favors the photocatalytic activity.



Scheme 12 Hole trapping by MTPM and simultaneous formation of an oxidation product (based on ref. 143).

to be the optimum to induce complete crystallization of the NT-TiO₂ into the anatase phase without traces of rutile. It was found that the presence of rutile is remarkably detrimental for the overall photocatalytic activity of the solid. Using as probe molecules one azo dye like Acid Orange 7 (AO7) and one non azo dye like MB, the photocatalytic activity of this surface of ordered arrays of NT-TiO₂ was established and compared to that of a film of independent P25 nanoparticles.¹⁴⁵ It was observed that the photocatalytic activity of the P25 film was significantly lower than that of analogous films of NT-TiO₂.¹⁴⁵ Moreover the photocatalytic activity of the ordered NT-TiO₂ layers increases with the layer thickness.¹⁴⁵ Although the authors suggest that the higher efficiency of the ordered tubes, as compared to P25 film, is due to an optimized photocatalyst geometry that favors substrate diffusion and diminishes the required charge carriers diffusion path, no experimental evidence supporting this claim was given. Moreover, the proposal that the UV light is absorbed exclusively by the photocatalyst in the region in which the dye exhibits an absorption minimum is questionable. Normally one would have expected that photocatalysis is initiated by light absorption from the dye followed by electron injection from the dye in its excited state into the semiconductor conduction band.

Although, the number of examples reporting the specific features of photocatalyst having micrometric NT-TiO₂ morphology are still quite limited and many more examples are desirable, from the existing data it can be anticipated that the potential of these structures in photocatalysis is very large and promising in order to enhance the photocatalytic activity just by changing the shape and dimensions of the titania particles from conventionally spherical.

6. Titania structuring in the submillimetric length scale: photonic crystals as photocatalyst

Because less than a few percent of the solar photons can be absorbed by powdered anatase photocatalyst, considerable efforts have been made from a chemical point of view trying to modify the composition of TiO₂ in such a way that anatase

light absorption can be extended into the visible region. As commented on in the Introduction, doping and metal incorporation are typical examples of this approach. In addition to this methodology based on chemistry, one physical approach could be to increase the optimum light path, producing the entrapment of the light into the material. This methodology will promote light absorption, particularly for photons on the red side of the absorption inset.

Light absorption by the photocatalyst produces charge separation (Scheme 13). In contrast, those wavelengths that have lower energy than the band gap cannot be absorbed and therefore they will be reflected scattered and/or transmitted by the powder. However, on top of this necessary condition imposed by the relative energy of photons and band gap, it exists a probability associated with the electron transition that is related to the specific absorptivity of the material at a specific wavelength. In other words, energetics is a prerequisite for light absorption but other considerations related to the probability of the electronic transition also need to be considered. Photonic crystals serve to promote light absorption by increasing the effective light path through the material.^{146–151} In this way, photonic crystals act by increasing the apparent specific absorption coefficient of the material for those wavelengths matching the dimensions of the crystal.

In a photonic crystal the space is ordered in such a way that the light that enters in the crystal is trapped inside by a multitude of reflections and diffractions making light escape impossible. In order to produce this effect, the dimensions of the periodic dielectric constant field in the photonic crystal have to be commensurate with the wavelength of the trapped light. For this reason, photonic crystals have to be made of films having void dimensions between 0.3–0.8 μm corresponding to any of the visible wavelengths spatially ordered in a regular way expanding to the millimetric length scale. Thus, photonic crystals are based on the spatial structuring of titania in the submillimetric length scale.

Since the trapped light can not escape out of the crystal the probability that light absorption and charge separation occurs is considerably favored particularly at the onset of the absorption band where the specific absorption of the material is very low. Instead of allowing the photon to escape from the material, the photonic crystal arrangement increases the probability of electronic excitation by increasing the light/photocatalyst contact time. The fundamental of a photonic crystal is the structuring of the space creating a periodic dielectric constant field in the length scale of the visible light wavelength.^{150,152–154} This spatial structuring produces coherent Bragg diffraction patterns that forbid light of the corresponding wavelength to propagate through the material. At the Bragg diffraction frequencies, photons propagate with strongly reduced velocity so they are called *slow* photons. If



Scheme 13 Application of the photonic crystal concept in an inverse opal configuration to increase the effective light path through the photocatalyst increasing the probability of charge separation.

the energy of the slow photons overlaps with the absorption of the material, (even with very weak absorption) then the enhancement of the light absorption occurs as a consequence of the increase of the effective optical path length through the material.

Ozin and coworkers have used the physical approach to slow down photons and increase the photocatalytic activity of TiO_2 .¹⁵⁵ Thus, these authors prepared an inverse opal constituted by anatase nanocrystals ordered around monodisperse empty spheres of dimensions from 280 to 500 nm. The dimension of the sphere creates a *light stop band* at the wavelength corresponding to the dimensions of the spheres. To test the photocatalytic activity enhancement of this inverse photonic crystal, MB was used as a probe in the absence of solvent.¹⁵⁵ Studies with monochromatic light but also with polychromatic visible light were carried out to determine the influence of the void diameter in the red or in the blue side of the anatase optical absorption. Comparative photocatalytic experiments with unstructured TiO_2 films were carried out at similar surface coverage for which the absence of dye multilayer or aggregates can be ensured. For monochromatic 370 nm irradiation, the influence of the void dimensions of the inverse opals can lead to a decrease in the photocatalytic activity due to light reflection (for films with a void size of 370 nm) or to an enhancement of the photocatalytic activity when 370 nm corresponds to a somewhat longer length than the void size of the opal (films with void size of 340 nm). Furthermore, the enhancement factor of the photocatalytic efficiency depends on the angle of the incident light following the expected relationship for the Bragg equation.¹⁵⁵ For the polychromatic white light irradiation, it was also observed that the optimum void dimension to obtain the maximum enhancement of the photocatalytic activity was 300 nm for which an enhancement factor of 2.3 was determined for films with photonic crystal structuring with respect to unstructured TiO_2 nanoparticles. Interestingly, the photocatalytic activity of a mesostructured TiO_2 film prepared by demolition of an inverse opal matrix crashing several samples and using the resulting powder to prepare a non-structured film was the same as an analogous film made of conventional TiO_2 nanoparticles.¹⁵⁵ This indicates that the intrinsic photocatalytic activity of the TiO_2 particles forming the inverse opal structure is the one that should be expected for conventional TiO_2 .

The practicality of inverse opal films constituted by anatase nanoparticles as an efficient photocatalyst depends upon the level of structural disorder that can be tolerated while maintaining the enhancement effect. Since structuring, dislocation and other defects are inherent to a 3D crystal, it is of interest to determine through a systematic study the influence of the degree of disorder on the photocatalytic activity enhancement. This study has been carried out by Ozin and coworkers using the photodegradation of MB as a probe to test the photocatalytic efficiency of titania inverse opal having some disorder.¹⁵⁶ The disorder in the crystal was purposely introduced by preparing films substituting in the system different proportions of 150 nm spheres by spheres of 180 or 210 nm (Scheme 14). Comparing the photocatalytic activity of the films prepared with monodisperse 150 nm latex spheres, the enhancement of the photocatalytic activity decreases gradually with the struc-



Scheme 14 Schematic representation of the defects in the photonic crystal made of latex spheres induced by the introduction of larger spheres in a perfect opal film (based on ref. 156).

tural defect and a point is reached in which no advantages with respect to the unstructured film of conventional monocrystalline TiO_2 is achieved. For a film of polystyrene opal template, it was observed that doping with larger spheres introduces defects that destroy the long range order much more significantly than when doping with smaller spheres.¹⁵⁶ In general, the band of the inverse opal structure corresponding to the Bragg diffraction is much more sensitive to defects than that of the polystyrene templates, probably because disorder of the template is magnified during the replica of the template to form inverse opal.

Nevertheless, a photodegradation enhancement of about 50% respect to unstructured films can be easily achieved even for inverse opals having a considerable degree of disorder.¹⁵⁶ In any case, defects produced by the presence of larger spheres (210 nm as compared to 180 nm) influence strongly reducing the photocatalytic activity much more drastically than defects introduced by spheres with sizes more similar to those constituting the perfect opal.

Besides the opal structure, Meseguer *et al.* have expanded the concept to the photonic sponge.¹⁵⁷ In this case instead of having a mononodal distribution of spherical voids of a single diameter, the sponge has an appropriate distribution of different size spheres in such a way that the entire wavelength range in a particular spectral region can be trapped.¹⁵⁷ This means that, in contrast to the classical photonic crystal, not only one particular wavelength, but most of the visible spectra can be trapped inside a photonic sponge. In this way, the photonic sponge should show enhanced photocatalytic activity no matter which excitation wavelengths or substrates are going to be used. These sponges are particularly useful for polychromatic light irradiation of colorless substrates for which TiO_2 should absorb photons.

A photonic sponge can be obtained by impregnation with P25 nanoparticles of a film constituted by a mixture of polystyrene latex spheres of different size in a proportion that compensate smaller *versus* larger diameters.¹⁵⁸ This proportion follows a geometry in which smaller spheres occupy the corners and empty spaces left among larger spheres in a close packing configuration.

The photocatalytic activity of a photonic sponge has been tested using succinonitrile as substrate and following the degradation course by IR spectroscopy.¹⁵⁸ Fig. 9 shows the decrease in the absorption intensity of the characteristic CH_2 stretching vibration band of succinonitrile at about 2990 cm^{-1} upon increase of the irradiation time.

Comparison with an analogous unstructured film made by P25 nanoparticles indicates that structuring the photonic sponge increases the photocatalytic activity by one order of magnitude. One interesting observation was that an increase of the film thickness of the photonic sponge can be

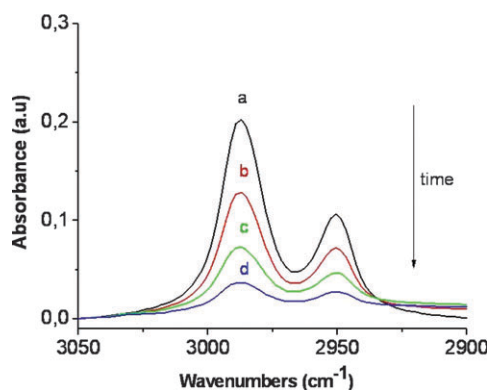


Fig. 9 Intensity decrease along the irradiation time of the CH₂ band characteristic of succinonitrile incorporated inside a TiO₂ photonic sponge (taken from ref. 158).

unfavorable for the photocatalytic activity of the film. This was interpreted assuming that for thick photonic sponge films the light is not able to penetrate through the whole layer and therefore the substrate located deep inside the layer can not be degraded due to the lack of light at this depth. Thus, there is an optimum larger thickness of about a few microns.

7. Conclusions and future prospects

Improvement of the photocatalytic activity of TiO₂ is absolutely necessary to implement real life application of photocatalysis. While the vast majority of the current approaches to effect the enhancement of the photocatalytic activity is based on modification of the chemical composition introducing various degrees of doping (chemical approaches), in the present account we have shown that control of the particle size and spatial organization of TiO₂ nanoparticles (physical approach) is also a powerful methodology to improve the photocatalytic efficiency. Recognition of this fact among the photocatalytic community will be of large importance to accelerate further development in this area. In this sense the independent development of the physical and chemical approaches to boost the photocatalytic activity is clear at the present stage. It can be easily anticipated that the near future developments will combine all the possible methodologies. In this regard it is remarkable the scarcity of the number of studies on spatial structuring of TiO₂ that use doped or chemically modified titania. Doping and spatial structuring combined together can produce a new generation of materials with sufficiently high photocatalytic efficiency under visible and solar light irradiation so that commercial implementation of photocatalysis can be brought to fruition.

Also, it can be expected that host–guest supramolecular chemistry concepts will be applied on top of spatial structuring and chemical doping. Thus, one further degree of complexity will involve systems in which a guest is present inside a porous titania with appropriate shape, dimensions and spatial ordering to promote the photocatalytic efficiency of the semiconductor by photosensitization and electron/hole injection. In this case, the guest has to be persistent enough to be stable during the operation of the photocatalytic system.

Acknowledgements

Authors thank CICYT (Project MAT2006-14274-C02-01) and (MAT20070157) for financial supports. Carmela Aprile thanks the Spanish Ministry of Education for a research associate Juan de la Cierva contract.

References

- 1 M. Kitano, M. Matsuoka, M. Ueshima and M. Anpo, *Appl. Catal., A*, 2007, **325**, 1.
- 2 H. B. Thu, M. Karkmaz, E. Puzenat, C. Guillard and J.-M. Herrmann, *Research on Chemical Intermediates*, 2005, **31**, 449.
- 3 M. Schiavello, *Heterogeneous Photocatalysis*, Kluwer Academic Publishers, Dordrecht, 1997.
- 4 M. Schiavello, *NATO ASI Series, Series C: Mathematical and Physical Sciences*, 1988, **237**, 351.
- 5 O. Legrini, E. Oliveros and A. M. Braun, *Chem. Rev.*, 1993, **93**, 671.
- 6 M. A. Fox and M. T. Dulay, *Chem. Rev.*, 1993, **93**, 341.
- 7 D. F. Ollis and H. Al-Ekabi, in *Photocatalytic Purification and Treatment of Water and Air*, ed. D. F. Ellis and H. Al-Ekabi, Elsevier, Amsterdam, 1993.
- 8 O. M. Alfano, D. Bahnemann, A. E. Cassano, R. Dillert and R. Goslich, *Catal. Today*, 2000, **58**, 199.
- 9 D. Bahnemann, *Handbook of Environmental Chemistry*, 1999, **2**, 285.
- 10 D. Bahnemann, *Sol. Energ.*, 2004, **77**, 445.
- 11 D. Bahnemann, J. Cunningham, M. A. Fox, E. Pelizzetti, P. Pichat and N. Serpone, *Aquat. Surf. Photochem.*, 1994, 261.
- 12 J. M. Herrmann, *Catal. Today*, 1995, **24**, 157.
- 13 J. M. Herrmann, *Catal. Today*, 1999, **53**, 115.
- 14 J. M. Herrmann, *Catal. Sci. Ser.*, 1999, **1**, 171.
- 15 M. R. Hoffmann, S. T. Martin, W. Choi and D. W. Bahnemann, *Chem. Rev.*, 1995, **95**, 69.
- 16 A. L. Linsebigler, G. Lu and J. T. Yates, Jr, *Chem. Rev.*, 1995, **95**, 735.
- 17 P. Pichat, C. Guillard, C. Maillard, L. Amalric and J. C. D'Oliveira, *Trace Met. Environm.*, 1993, **3**, 207.
- 18 A. Wold, *Chem. Mater.*, 1993, **5**, 280.
- 19 J. Cunningham, G. Al-Sayyed, P. Sedlak and J. Caffrey, *Catal. Today*, 1999, **53**, 145.
- 20 H. Yamashita, M. Takeuchi and M. Anpo, *Encyclopedia of Nanoscience and Nanotechnology*, 2004, **10**, 639.
- 21 H. Kisch and W. Macyk, *ChemPhysChem*, 2002, **3**, 399.
- 22 R. Bacsá, J. Kiwi, T. Ohno, P. Albers and V. Nadochenko, *J. Phys. Chem. B*, 2005, **109**, 5994.
- 23 K. E. Karakitsou and X. E. Verykios, *J. Phys. Chem.*, 1993, **97**, 1184.
- 24 J. Kiwi and M. Gratzel, *J. Phys. Chem.*, 1986, **90**, 637.
- 25 J. Kiwi and C. Morrison, *J. Phys. Chem.*, 1984, **88**, 6146.
- 26 Z. Jin, X. Zhang, Y. Li, S. Li and G. Lu, *Catal. Commun.*, 2007, **8**, 1267.
- 27 O. Ozcan, F. Yukruk, E. U. Akkaya and D. Uner, *Appl. Catal., B*, 2007, **71**, 291.
- 28 Z. Jin, X. Zhang, G. Lu and S. Li, *J. Mol. Catal. A: Chem.*, 2006, **259**, 275.
- 29 R. Abe, K. Sayama and H. Arakawa, *J. Photochem. Photobiol., A*, 2004, **166**, 115.
- 30 L.-C. Chen, C.-M. Huang and F.-R. Tsai, *J. Mol. Catal. A: Chem.*, 2007, **265**, 133.
- 31 F. Fresno, C. Guillard, J. M. Coronado, J.-M. Chovelon, D. Tudela, J. Soria and J.-M. Herrmann, *J. Photochem. Photobiol., A*, 2005, **173**, 13.
- 32 L. Ge and M. Xu, *Mater. Sci. Eng., B*, 2006, **131**, 222.
- 33 N. Serpone, *J. Phys. Chem. B*, 2006, **110**, 24287.
- 34 J. C. Colmenares, M. A. Aramendia, A. Marinas, J. M. Marinas and F. J. Urbano, *Appl. Catal., A*, 2006, **306**, 120.
- 35 S. Rengaraj and X. Z. Li, *J. Mol. Catal. A: Chem.*, 2006, **243**, 60.
- 36 W. Choi, A. Termin and M. R. Hoffmann, *J. Phys. Chem.*, 1994, **98**, 13669.
- 37 W. Choi, A. Termin and M. R. Hoffmann, *Angew. Chem.*, 1994, **106**, 1148.

- 38 C. Bauer, G. Boschloo, E. Mukhtar and A. Hagfeldt, *J. Phys. Chem. B*, 2002, **106**, 12693.
- 39 J. He, J. Zhao, T. Shen, H. Hidaka and N. Serpone, *J. Phys. Chem. B*, 1997, **101**, 9027.
- 40 P. V. Kamat, S. Das, K. G. Thomas and M. V. George, *Chem. Phys. Lett.*, 1991, **178**, 75.
- 41 D. I. Kreller and P. V. Kamat, *J. Phys. Chem.*, 1991, **95**, 4406.
- 42 Y. Ohsaki, N. Masaki, T. Kitamura, Y. Wada, T. Okamoto, T. Sekino, K. Niihara and S. Yanagida, *Phys. Chem. Chem. Phys.*, 2005, **7**, 4157.
- 43 J. E. Kroeze, T. J. Savenije and J. M. Warman, *J. Am. Chem. Soc.*, 2004, **126**, 7608.
- 44 A. Kay, R. Humphry-Baker and M. Graetzel, *J. Phys. Chem.*, 1994, **98**, 952.
- 45 Y.-J. Lin, S.-L. Tseng, W.-J. Huang and W.-J. Wu, *J. Environ. Sci. Health, Part B*, 2006, **41**, 1143.
- 46 T. Okato, T. Sakano and M. Obara, *Phys. Rev. B: Condens. Matter Mater. Phys.*, 2005, **72**, 115124/1.
- 47 R. Asahi, T. Morikawa, T. Ohwaki, K. Aoki and Y. Taga, *Science*, 2001, **293**, 269.
- 48 Y. Cong, F. Chen, J. Zhang and M. Anpo, *Chem. Lett.*, 2006, **35**, 800.
- 49 C. Di Valentin, G. Pacchioni and A. Selloni, *Chem. Mater.*, 2005, **17**, 6656.
- 50 D. Li, H. Haneda, N. K. Labhsetwar, S. Hishita and N. Ohashi, *Chem. Phys. Lett.*, 2005, **401**, 579.
- 51 T. Ohno, T. Tsubota, M. Toyofuku and R. Inaba, *Catal. Lett.*, 2004, **98**, 255.
- 52 S. Sakthivel, M. Janczarek and H. Kisch, *J. Phys. Chem. B*, 2004, **108**, 19384.
- 53 T. Tachikawa, S. Tojo, K. Kawai, M. Endo, M. Fujitsuka, T. Ohno, K. Nishijima, Z. Miyamoto and T. Majima, *J. Phys. Chem. B*, 2004, **108**, 19299.
- 54 M. Mrowetz, W. Balcerski, A. J. Colussi and M. R. Hoffmann, *J. Phys. Chem. B*, 2004, **108**, 17269.
- 55 H. Liu and L. Gao, *J. Am. Ceram. Soc.*, 2004, **87**, 1582.
- 56 S. Sakthivel and H. Kisch, *ChemPhysChem*, 2003, **4**, 487.
- 57 S.-Z. Chu, S. Inoue, K. Wada, D. Li and J. Suzuki, *Langmuir*, 2005, **21**, 8035.
- 58 M. Anpo, H. Yamashita, Y. Ichihashi, Y. Fujii and M. Honda, *J. Phys. Chem. B*, 1997, **101**, 2632.
- 59 G. Lassaletta, A. Fernandez, J. P. Espinos and A. R. Gonzalez-Elipe, *J. Phys. Chem.*, 1995, **99**, 1484.
- 60 C. Kormann, D. W. Bahnemann and M. R. Hoffmann, *J. Phys. Chem.*, 1988, **92**, 5196.
- 61 S. H. Tolbert, A. B. Herhold, C. S. Johnson and A. P. Alivisatos, *Phys. Rev. Lett.*, 1994, **73**, 3266.
- 62 A. Henglein, *Chem. Rev.*, 1989, **89**, 1861.
- 63 M. Alvaro, E. Carbonell, V. Fornes and H. Garcia, *ChemPhysChem*, 2006, **7**, 200.
- 64 D. C. Hurum, K. A. Gray, T. Rajh and M. C. Thurnauer, *J. Phys. Chem. B*, 2005, **109**, 977.
- 65 D. C. Hurum, A. G. Agrios, K. A. Gray, T. Rajh and M. C. Thurnauer, *J. Phys. Chem. B*, 2003, **107**, 4545.
- 66 Z. Ding, G. Q. Lu and P. F. Greenfield, *J. Phys. Chem. B*, 2000, **104**, 4815.
- 67 J. Klaas, G. Schulz-Ekloff and N. I. Jaeger, *J. Phys. Chem. B*, 1997, **101**, 1305.
- 68 X. S. Zhao, G. Q. Lu and G. J. Millar, *J. Porous Mater.*, 1996, **3**, 61.
- 69 G. Grubert, M. Stockenhuber, O. P. Tkachenko and M. Wark, *Chem. Mater.*, 2002, **14**, 2458.
- 70 G. Grubert, M. Wark, N. I. Jaeger, G. Schulz-Ekloff and O. P. Tkachenko, *J. Phys. Chem. B*, 1998, **102**, 1665.
- 71 R. M. Barrer, *Zeolites and Clay Minerals as Sorbents and Molecular Sieves*, Academic Press, London, 1978.
- 72 D. W. Breck, *Zeolite Molecular Sieves: Structure, Chemistry, and Use*, Wiley-Interscience, New York, 1974.
- 73 A. Corma, F. Rey, J. Rius, M. J. Sabater and S. Valencia, *Nature*, 2004, **431**, 287.
- 74 B. W. Wojciechowski and A. Corma, *Catalytic Cracking: Catalysts, Chemistry, and Kinetics*, Khimiya, Moscow, 1990.
- 75 L. B. McCusker and C. Baerlocher, *Stud. Surf. Sci. Catal.*, 2001, **137**, 37.
- 76 (a) A. Corma, M. J. Diaz-Cabanas, F. Rey, S. Nicolopoulos and K. Boulahya, *Chem. Commun.*, 2004, **12**, 1356; (b) A. Corma, M. J. Diaz-Cabanas, J. L. Jorda, C. Martinez and Manuel Moliner, *Nature*, 2006, **443**, 842.
- 77 A. Corma and H. Garcia, *Chem. Commun.*, 2004, 1443.
- 78 S. H. Bossmann, C. Turro, C. Schnabel, M. R. Pokhrel, L. M. Payawan, Jr, B. Baumeister and M. Woerner, *J. Phys. Chem. B*, 2001, **105**, 5374.
- 79 T. Kapias and R. F. Griffiths, *J. Hazard. Mater.*, 2005, **119**, 41.
- 80 P. K. Roy, A. Bhatt and C. Rajagopal, *J. Hazard. Mater.*, 2003, **102**, 167.
- 81 E. H. Fochtman, C. Swanstrom and T. Cashen, *Environ. Prog.*, 1988, **7**, 112.
- 82 X. Liu, K. K. Iu and J. K. Thomas, *J. Chem. Soc., Faraday Trans.*, 1993, **89**, 1861.
- 83 X. Liu, K. K. Iu and J. K. Thomas, *Chemical. Phys. Lett.*, 1992, **195**, 163.
- 84 A. Corma and H. Garcia, *Chem. Rev.*, 2002, **102**, 3837.
- 85 A. Zecchina, S. Bordiga, C. Lamberti, G. Ricchiardi, C. Lamberti, G. Ricchiardi, D. Scarano, G. Petrini, G. Leofanti and M. Mantegazza, *Catal. Today*, 1996, **32**, 97.
- 86 F. Geobaldo, S. Bordiga, A. Zecchina, E. Giamello, G. Leofanti and G. Petrini, *Catal. Lett.*, 1992, **16**, 109.
- 87 M. Wark, G. Grubert, M. Warnken, G. Schulz-Ekloff, M. Ganschow, Y. Rohlfing, T. Bogdahn-Rai and D. Wöhrle, *Appl. Mineral.*, 2000, **1**, 253.
- 88 G. Cosa, M. S. Galletero, L. Fernandez, F. Marquez, H. Garcia and J. C. Scaiano, *New J. Chem.*, 2002, **26**, 1448.
- 89 S. Corrent, G. Cosa, J. C. Scaiano, M. S. Galletero, M. Alvaro and H. Garcia, *Chem. Mater.*, 2001, **13**, 715.
- 90 S. Zhang, N. Fujii and Y. Nosaka, *J. Mol. Catal. A: Chem.*, 1998, **129**, 219.
- 91 T. V. Choudhary, *Ind. Eng. Chem. Res.*, DOI: 10.1021/ie061617d.
- 92 C. Song, *Catal. Today*, 2003, **86**, 211.
- 93 (a) A. Chica, A. Corma and M. E. Domine, *J. Catal.*, 2006, **242**, 299; (b) M. Alvaro, E. Carbonell and H. Garcia, *Appl. Catal., B*, 2004, **51**, 195.
- 94 M. N. Chretien, *Pure Appl. Chem.*, 2007, **79**, 1.
- 95 F. X. Llabres i Xamena, P. Calza, C. Lamberti, C. Prestipino, A. Damin, S. Bordiga, E. Pelizzetti and A. Zecchina, *J. Am. Chem. Soc.*, 2003, **125**, 2264.
- 96 Y. I. Kim, S. W. Keller, J. S. Krueger, E. H. Yonemoto, G. B. Saupe and T. E. Mallouk, *J. Phys. Chem. B*, 1997, **101**, 2491.
- 97 Y. I. Kim, R. L. Riley, M. J. Huq, S. Salim, A. N. Le and T. E. Mallouk, *Mater. Res. Soc. Symp. Proceed.*, 1991, **233**, 145.
- 98 J. S. Krueger, C. Lai, Z. Li, J. E. Mayer and T. E. Mallouk, *J. Inclusion Phenom. Mol. Recognit.*, 1990, 365.
- 99 H. Garcia and H. D. Roth, *Chem. Rev.*, 2002, **102**, 3947.
- 100 P. K. Dutta and W. Turbeville, *J. Phys. Chem.*, 1992, **96**, 9410.
- 101 W. Turbeville, D. S. Robins and P. K. Dutta, *J. Phys. Chem.*, 1992, **96**, 5024.
- 102 J. A. Incavo and P. K. Dutta, *J. Phys. Chem.*, 1990, **94**, 3075.
- 103 S. H. Bossmann, S. Jockusch, P. Schwarz, B. Baumeister, S. Goeb, C. Schnabel, L. Payawan, Jr, M. R. Pokhrel, M. Woerner, A. M. Braun and N. J. Turro, *Photochem. Photobiol. Sci.*, 2003, **2**, 477.
- 104 S. H. Bossmann, N. Shahin, H. Le Thanh, A. Bonfill, M. Worner and A. M. Braun, *ChemPhysChem*, 2002, **3**, 401.
- 105 G. Cosa, M. N. Chretien, M. S. Galletero, V. Fornes, H. Garcia and J. C. Scaiano, *J. Phys. Chem. B*, 2002, **106**, 2460.
- 106 M. Alvaro, M. N. Chretien, V. Fornes, M. S. Galletero, H. Garcia and J. C. Scaiano, *J. Phys. Chem. B*, 2004, **108**, 16621.
- 107 K. Ikeue, H. Yamashita and M. Anpo, *Electrochemistry*, 2002, **70**, 402.
- 108 H. Yamashita, K. Ikeue and M. Anpo, *ACS Symp. Ser.*, 2002, **809**, 330.
- 109 J. Zhang, Y. Hu, M. Matsuoka, H. Yamashita, M. Minagawa, H. Hidaka and M. Anpo, *J. Phys. Chem. B*, 2001, **105**, 8395.
- 110 K. Ikeue, H. Yamashita, M. Anpo and T. Takewaki, *J. Phys. Chem. B*, 2001, **105**, 8350.
- 111 K. Ikeue, H. Yamashita and M. Anpo, *Chem. Lett.*, 1999, 1135.
- 112 M. Anpo, S. Higashimoto and M. Matsuoka, *Eco Ind.*, 1999, **4**, 11.

- 113 H. Yamashita, Y. Fujii, Y. Ichihashi, S. G. Zhang, K. Ikeue, D. R. Park, K. Koyano, T. Tatsumi and M. Anpo, *Catal. Today*, 1998, **45**, 221.
- 114 M. Anpo, H. Yamashita, K. Ikeue, Y. Fujii, Y. Ichihashi, S. G. Zhang, D. R. Park, S. Ehara, S.-E. Park, J.-S. Chang and J. W. Yoo, *Stud. Surf. Sci. Catal.*, 1998, **114**, 177.
- 115 H. Yamashita, Y. Ichihashi, S. G. Zhang, Y. Matsumura, Y. Souma, T. Tatsumi and M. Anpo, *Appl. Surf. Sci.*, 1997, **121/122**, 305.
- 116 H. Yamashita, Y. Ichihashi, M. Anpo, M. Hashimoto, C. Louis and M. Che, *J. Phys. Chem.*, 1996, **100**, 16041.
- 117 J. C. Vartuli, C. T. Kresge, M. E. Leonowicz, A. S. Chu, S. B. McCullen, I. D. Johnson and E. W. Sheppard, *Chem. Mater.*, 1994, **6**, 2070.
- 118 C. T. Kresge, M. E. Leonowicz, W. J. Roth, J. C. Vartuli and J. S. Beck, *Nature*, 1992, **359**, 710.
- 119 J. S. Beck, J. C. Vartuli, W. J. Roth, M. E. Leonowicz, C. T. Kresge, K. D. Schmitt, C. T. W. Chu, D. H. Olson, E. W. Sheppard, S. B. McCullen, J. B. Higgins and J. L. Schenkler, *J. Am. Chem. Soc.*, 1992, **114**, 10834.
- 120 C. Boissiere, D. Grosso, B. Smarsly, T. Brezesinski, S. Lepoutre, L. Nicole, J. C. V. Marcos, M. Antonietti and C. Sanchez, *Mater. Res. Soc. Symp. Proceed.*, 2005, **847**, 135.
- 121 S. Polarz and M. Antonietti, *Chem. Commun.*, 2002, 2593.
- 122 C. G. Goltner and M. Antonietti, *Adv. Mater.*, 1997, **9**, 431.
- 123 E. L. Crepaldi, G. J. de Soler-Illia, D. Grosso, F. Cagnol, F. Ribot and C. Sanchez, *J. Am. Chem. Soc.*, 2003, **125**, 9770.
- 124 D. Grosso, G. J. d. A. A. Soler-Illia, E. L. Crepaldi, F. Cagnol, C. Sinturel, A. Bourgeois, A. Brunet-Bruneau, H. Amenitsch, P. A. Albouy and C. Sanchez, *Chem. Mater.*, 2003, **15**, 4562.
- 125 M. H. Bartl, S. W. Boettcher, K. L. Frindell and G. D. Stucky, *Acc. Chem. Res.*, 2005, **38**, 263.
- 126 J. Tang, Y. Wu, E. W. McFarland and G. D. Stucky, *Chem. Commun.*, 2004, 1670.
- 127 M. Andersson, H. Birkedal, N. R. Franklin, T. Ostomel, S. Boettcher, A. E. C. Palmqvist and G. D. Stucky, *Chem. Mater.*, 2005, **17**, 1409.
- 128 M. Alvaro, C. Aprile, M. Benitez, E. Carbonell and H. Garcia, *J. Phys. Chem. B*, 2006, **110**, 6661.
- 129 M. Gaertner, V. Dremov, P. Mueller and H. Kisch, *Chem-PhysChem*, 2005, **6**, 714.
- 130 M. Fagnoni, D. Dondi, D. Ravelli and A. Albini, *Chem. Rev.*, 2007, **107**, 2725.
- 131 L. Cermenati, C. Richter and A. Albini, *Chem. Commun.*, 1998, 805.
- 132 A. Maldotti, A. Molinari and R. Amadelli, *Chem. Rev.*, 2002, **102**, 3811.
- 133 A. Maldotti, A. Molinari, G. Varani, M. Lenarda, L. Storaro, F. Bigi, R. Maggi, A. Mazzacani and G. Sartori, *J. Catal.*, 2002, **209**, 210.
- 134 A. Molinari, R. Amadelli, L. Andreotti and A. Maldotti, *J. Chem. Soc., Dalton Trans.*, 1999, 1203.
- 135 P. Boarini, V. Carassiti, A. Maldotti and R. Amadelli, *Langmuir*, 1998, **14**, 2080.
- 136 A. Maldotti, A. Molinari, E. Carbonell and H. Garcia, unpublished results.
- 137 M. A. Carreon, S. Y. Choi, M. Mamak, N. Chopra and G. A. Ozin, *J. Mater. Chem.*, 2007, **17**, 82.
- 138 H. Li, Z. Bian, J. Zhu, Y. Huo, H. Li and Y. Lu, *J. Am. Chem. Soc.*, 2007, **129**, 4538.
- 139 J. T. McCann, M. Marquez and Y. Xia, *Nano Lett.*, 2006, **6**, 2868.
- 140 Z. Zhong, T.-P. Ang, J. Luo, H.-C. Gan and A. Gedanken, *Chem. Mater.*, 2005, **17**, 6814.
- 141 C. Xiong and K. J. Balkus, Jr, *Chem. Mater.*, 2005, **17**, 5136.
- 142 Z.-Y. Yuan and B.-L. Su, *Colloids Surf., A*, 2004, **241**, 173.
- 143 T. Tachikawa, M. Fujitsuka and T. Majima, *J. Phys. Chem. C*, 2007, **111**, 5259.
- 144 J. H. Park, S. Kim and A. J. Bard, *Nano Lett.*, 2006, **6**, 24.
- 145 J. M. Macak, M. Zlamal, J. Krysa and P. Schmuki, *Small*, 2007, **3**, 300.
- 146 T. Baba, *Nat. Photonics*, 2007, **1**, 11.
- 147 D. J. Norris, *Nat. Mater.*, 2007, **6**, 177.
- 148 D. A. B. Miller, *Nat. Mater.*, 2006, **5**, 83.
- 149 M. Egen, R. Zentel, P. Ferrand, S. Eiden, G. Maret and F. Caruso, *Photonic Cryst.*, 2004, 109.
- 150 N. Tetreault, H. Miguez and G. A. Ozin, *Adv. Mater.*, 2004, **16**, 1471.
- 151 N. Hall, *Chem. Commun.*, 2003, 2639.
- 152 A. Arsenault, F. Fleischhaker, G. von Freymann, V. Kitaev, H. Miguez, A. Mihi, N. Tetreault, E. Vekris, I. Manners, S. Aitchison, D. Perovic and G. A. Ozin, *Adv. Mater.*, 2006, **18**, 2779.
- 153 M. Wegener, K. Arnold, K. Busch, M. Deubel, C. Enkrich, D. Fenske, G. von Freymann, M. Hermatschweller, S. John, M. Kappes, A. Kaso, S. Linden, G. A. Ozin, S. Pereira, F. Perez-Willard, C. M. Soukoulis, N. Tetreault and S. Wong, *PMSE Preprints*, 2006, **94**, 97.
- 154 G. A. Ozin and S. M. Yang, *Adv. Funct. Mater.*, 2001, **11**, 95.
- 155 J. I. L. Chen, G. von Freymann, S. Y. Choi, V. Kitaev and G. A. Ozin, *Adv. Mater.*, 2006, **18**, 1915.
- 156 J. I. L. Chen, G. von Freymann, V. Kitaev and G. A. Ozin, *J. Am. Chem. Soc.*, 2007, **129**, 1196.
- 157 F. Ramiro-Manzano, P. Atienzar, I. Rodriguez, F. Meseguer, H. Garcia and A. Corma, *Chem. Commun.*, 2007, 242.
- 158 E. Carbonell, F. Ramiro-Manzano, F. Meseguer, A. Corma and H. Garcia, unpublished results.